https://doi.org/10.5194/esd-2020-35
Preprint. Discussion started: 20 July 2020


Earth System Dynamics Discussions

# Agricultural management effects on mean and extreme temperature trends

Aine M. Gormley-Gallagher[1], Sebastian Sterl[1,2,3], Annette L. Hirsch[4], Sonia I. Seneviratne[5], Edouard L. Davin[5], Wim Thiery[1,5]

[1]Department of Hydrology and Hydraulic Engineering, Vrije Universiteit Brussel, Brussels, 1050, Belgium
[2]Department of Earth and Environmental Sciences, KU Leuven, Leuven, Belgium
[3]Center for Development Research, University of Bonn, Bonn, Germany
[4]ARC Centre of Excellence for Climate Extremes, University of New South Wales, Sydney, Australia
[5]Institute for Atmospheric and Climate Science, ETH Zurich, Zurich, Switzerland

*Correspondence to*: Aine M. Gormley-Gallagher (a.gormley@ulster.ac.uk)

**Abstract.** Regression-based trend analysis is applied to observations and present-day ensemble simulations with the Community Earth System Model (CESM) version 1.2.2 to assess if this model overestimates warming trends because irrigation and conservation agriculture (CA) are excluded. At the regional scale, an irrigation- and CA-induced acceleration of the annual mean near-surface air temperature ($T_{2m}$) warming trends and the annual maximum daytime temperature (TXx) warming trends were evident. Estimation of the impact of irrigation and CA on the spatial average of the warming trends indicated that irrigation and CA have a pulse cooling effect on $T_{2m}$ and TXx, after which the warming trends increase at a greater rate than the control simulations. This differed at the local (subgrid) scale under irrigation where surface temperature cooling and the dampening of warming trends were both evident. As the local surface warming trends, in contrast to regional trends, do not account for atmospheric (water vapour) feedbacks, their dampening confirms the importance of atmospheric feedbacks (water vapour forcing) in explaining the enhanced regional trends. At the land surface, the positive radiative forcing signal is too weak to offset the local cooling from the irrigation-induced increase in the evaporative fraction. Our results underline that agricultural management has complex and nonnegligible impacts on the local climate and highlights the need to account for land management in climate projections.

## 1 Introduction

According to observational and global climate model (GCM) data, temperatures associated with hot extremes have increased consistent with global anthropogenic climate change (Sillmann and Croci-Maspoli, 2009; Donat et al., 2013a, 2013b; Hartmann et al., 2013; Pendergrass and Hartmann, 2014; Fischer and Knutti, 2015). However, hot spots of accelerated warming in annual maximum daytime temperature (TXx) relative to local mean temperature ($T_{2m}$) simulated by climate models from phase 5 of the World Climate Research Programme's (WCRP) Coupled Model Intercomparison Project (CMIP5) are spatially inconsistent with observations (Donat et al., 2017). This is particularly the case over southeast China,

https://doi.org/10.5194/esd-2020-35
Preprint. Discussion started: 20 July 2020


Earth System Dynamics Discussions

South America, north America and parts of Australia and Europe. In these regions, the modelled TXx warming from the midtwentieth century (1951–1980) to the late 20th/early 21st century (1981–2010) was greater than the modelled $T_{2m}$ warming. In contrast to the models, the observations showed that TXx warmed at a slower rate than $T_{2m}$. Further analysis of the CMIP5 ensemble over central Europe by Vogel et al. (2018) highlighted that several GCMs overestimate the observed negative correlation between summer precipitation and TXx, resulting in too strong future drying and associated increases in TXx under RCP8.5. This underlines the importance of a correct representation of land-atmosphere coupling for simulating changes in temperature extremes at regional scales. These discrepancies between multiple GCMs and observations raise the question as to whether these model results can be used to reliably project changes in local temperature extremes.

Agricultural land management techniques, including irrigation and conservation agriculture, can have a cooling effect on hot temperature extremes (Davin et al., 2014; Hirsch et al., 2017; Thiery et al., 2017, 2020; Hauser et al., 2019; Jia et al., 2019). Irrigation diverts surface and groundwater resources to agricultural land to increase crop production (Fereres and Soriano, 2007). The addition of this water to the land surface is balanced by the loss of water via runoff, deep percolation, soil storage and/or evapotranspiration (ET) (Fereres and Connor, 2004). Under drier conditions, less evaporative cooling leads to amplified warming because the energy budget becomes dominated by sensible heating instead of latent heating (Donat et al., 2017). If irrigation water is added to the surface, this increases soil moisture as well as latent heat flux over the summer months, leading to more evaporative cooling at the land surface. Thiery et al. (2017) used the Community Earth System Model version 1.2.2 (CESM1.2.2, hereafter referred to as CESM) to investigate the influence of irrigation on temperature extremes on a global scale. They found that irrigation induced strong cooling on irrigated pixels – an average of -0.78 K compared to a no-irrigation case – during the hottest day of the year.

Conservation agriculture (CA), which involves crop residue management, crop rotation (Carrer et al., 2018; Lombardozzi et al., 2018) and minimal or no tillage (Kassam et al., 2015), can create climate feedbacks due to the presence of a crop residue over CA land change both the radiative and hydrological properties at the surface (Davin et al., 2014). Hirsch et al. (2018) explored whether applying the no-till component of CA within the CESM improves the simulation of present-day climate. They found that the surface temperature response was influenced by three competing effects: (1) a surface albedo increase – which reduces the availability of energy for partitioning between the sensible and latent heat fluxes; (2) surface resistance increase (e.g. from mulch) – which reduces latent heat fluxes due to increased surface resistance to soil evaporation; and (3) soil moisture retention leading to enhanced transpiration. The local cooling response to CA was somewhat counteracted by grid-scale changes in climate over North America, Europe, and Asia because of negative atmospheric feedbacks. That is, the decrease in ET – both due to higher albedo and higher soil resistance – appeared to activate a decrease in cloud cover in the model that increased incoming radiation and therefore temperature.

https://doi.org/10.5194/esd-2020-35
Preprint. Discussion started: 20 July 2020


Earth System Dynamics Discussions

Interactions between crop albedo, irrigation, cloud formation and temperature were explored in a previous study by Hirsch et al. (2017). They found that the CESM tends to produce large cloud feedbacks over Central Europe, Central North America, North Asia, and South Asia when more energy is reflected at the surface. Irrigation-induced increases in latent heat fluxes over the boreal summer months were noted and revealed more evaporative cooling at the surface. The increase in the latent heat flux led to more water vapor in the lower atmosphere, which generated low-level clouds (see also Sherwood et al., 2017). This limited shortwave radiation and hence the amount of energy available at the surface because the increased cloud cover reflected more downward shortwave radiation above the cloud layer, resulting in surface cooling. This was enhanced by a corresponding decrease in sensible heat fluxes, reflecting the decrease in the amount of energy available at the surface and/or the increase in latent heating. More specifically, TXx locally decreased by up to 1–3°C. However, the cloud cover was sustained at the end of the growing season into the winter months. This, combined with the suspension of land management activities at this time, led to enhanced downward longwave radiation – and subsequently, additional warming during cold periods.

The importance of soil moisture-temperature coupling and its mechanisms controlling the regional amplification of extreme temperatures was assessed by Vogel et al. (2017) using models that contributed to the Global Land-Atmosphere Coupling Experiment (GLACE)-CMIP5 project, which aims to quantify soil moisture-climate interactions (Seneviratne et al., 2013). Vogel et al. (2017) describe the processes leading to regional amplifications of temperature extremes as follows. In simulations with increased soil moisture, the latent heat flux increases, as well as precipitation and cloud cover. Subsequently, net shortwave radiation decreases, followed by a temperature decline; however, an increase in net longwave radiation (mainly due to cloud cover) can counteract this effect, meaning that the net effect on radiation would be minor. Moreover, their results corroborated the previously described theory of Seneviratne et al. (2010) that the impacts of soil moisture on surface climate are strongest in transitional climate regimes between dry and wet climates.

The regions where the hot spots of accelerated TXx warming are inconsistent with observations are somewhat spatially correlated with the regions where CA and irrigation are extensive (Donat et al., 2017). Considering this, and the potential cooling effect of irrigation and CA on climate (Thiery et al., 2017), it is possible that the overestimated warming trends are because the models exclude the effect of agricultural management techniques on temperature. It remains challenging to resolve this, however, because it is difficult to separate land management from other effects in GCMs – particularly natural climate variability (Cook et al., 2015). The question remains as to whether the inclusion of land management practices in GCMs will improve the estimation of warming rates trends.

The goal of this study is thus to test the hypothesis that CESM version 1.2.2overestimates warming trends in some regions because irrigation and CA are excluded. That is, warming rates are hypothesised to decline – showing signs of cooling, in

https://doi.org/10.5194/esd-2020-35
Preprint. Discussion started: 20 July 2020


Earth System Dynamics Discussions

irrigation- and CA-affected regions when climate models do account for a theoretical constant level of these land management practices. To realise this goal, the following three objectives were formulated: (1) Determine spatial warming rates using GCM simulations that account for irrigation and CA and inspect whether CESM overestimates warming trends; (2) Compare the observed rates of warming to the modelled rates of warming for irrigated and CA pixels, as well as non-irrigated and non-CA pixels; and (3) Estimate the impact of irrigation on the spatial average of the warming rates over time (1981-2010) for all land, selected regions, and irrigated and CA pixels.

## 2 Materials and Methods

### 2.1 Irrigation and conservation agriculture implementation in CESM

To assess the influence of a theoretical constant level of either irrigation or CA on mean and extreme temperatures, we use the Community Earth System Model (CESM) version 1.2.2, which has contributed output to CMIP5 (Hurrell et al., 2013). The CESM atmospheric model was version 5.3 of the Community Atmosphere Model (CAM5.3) while the land surface model was version 4.0 of the Community Land Model (CLM4). Sea surface temperatures and sea ice fractions were prescribed from the data set described by Hurrell et al. (2008).

We analyse the control (1) and experimental (2) simulations presented in Thiery et al. (2017) for irrigation and in Hirsch et al. (2018) for CA. This set consists of three 5-member ensembles.

The first ensemble, the control (CTL), was set up to capture land-atmosphere components within a framework akin to that of the Atmospheric Model Intercomparison Project (AMIP). The period 1976-2010 was simulated with a horizontal pixel resolution of 0.9° latitude × 1.25° longitude. The first 5 years were discarded as spin-up, with trends evaluated for the period 1981-2010. On 1 January 1976, small random perturbations of $10^{-14}$ K were applied to the initial atmospheric temperature conditions. To focus on the influence of land–atmosphere interactions, rather than ocean–atmosphere feedbacks on the climate system, sea surface temperatures and sea ice fractions were prescribed from the data set described by Hurrell et al. (2008). Greenhouse gas concentrations were also prescribed from measurements, and satellite-based observations of vegetation phenology were imposed in CLM4.

The second ensemble, the irrigation (IRR) ensemble, follows an identical setup as the CTL experiment except that the interactive irrigation module in CLM4 was enabled. As described by Oleson et al. (2013), the irrigation parameterization in CLM4 divides the cropland area of each grid cell into non-irrigated and irrigated fractions corresponding to the portions that are equipped for irrigation – in accordance with Siebert et al.'s (2005) global map of irrigated areas (Figure 1a). The area of irrigated cropland in each grid cell is assigned as the smaller of the grid cells total cropland area and its area equipped for irrigation. What remains of the cropland area in the grid cell is regarded as non-irrigated cropland. It is important to note that

https://doi.org/10.5194/esd-2020-35
Preprint. Discussion started: 20 July 2020


Earth System Dynamics Discussions

implementation of transient irrigation was technically not possible in the CESM version 1.2, despite transient area equipped for irrigation data being available (Siebert et al., 2005), and therefore trends in the forcing are not considered.

The third ensemble, the CA ensemble, also follows the CTL experiment setup, but in this case the most likely distribution of CA was applied based on the CA dataset developed by Prestele et al. (2018). By splitting the existing CLM crop plant functional types (PFT) into a fraction under conservation agriculture and a fraction under conventional management, both forms of management are possible within a grid cell. Although the crop residue is assumed present all year, the implementation ensures that the increased soil albedo effect on the total surface albedo is dampened during the growing season by the inclusion of canopy cover (Hirsch et al., 2018). Implementation of transient CA, however, was not possible due to data limitation as only a static CA map was available; hence we study a theoretical constant level of CA.

In addition, land masks were used to define and analyse: (1) all land pixels; (2) irrigated pixels only (where grid cells have a nonzero irrigated fraction); (3) CA pixels (the grid cells with a nonzero CA fraction) and (4) those regions of the Special Report on Managing the Risks of Extreme Events and Disasters to Advance Climate Change Adaptation (SREX) (IPCC, 2013) where irrigation and CA is extensive (Figure 1). The spatial points outside these masks as well as missing values in the observations were excluded (as 'NaN' values). These masks were applied to the investigations undertaken in this study. As the observational datasets (see below) were remapped to the model grid, this meant the same land masks (excluding Antarctica) could be used for each dataset.

### 2.2 Observational datasets

For evaluation purposes, observational datasets for annual mean $T_{2m}$ with a spatial resolution of $0.5^{\circ} \times 0.5^{\circ}$ for the same time period were obtained from the Climate Research Unit (CRU) (Harris et al., 2014). Annual mean TXx observational datasets were obtained from the daily Global Historical Climatology Network extremes data set (GHCNDEX) (Donat et al., 2013a) and the Hadley Centre extremes data set (HadEX2) (Donat et al., 2013b) with a spatial resolution of $2.5^{\circ} \times 2.5^{\circ}$. All observational products were regridded to the CESM resolution using second-order conservative remapping (Jones, 1999). Thiery et al. (2017) and Hirsch et al. (2018) previously evaluated how the IRR and CA experiments alter the skill of CESM simulations (in terms of their agreement with observations). Thiery et al. (2017) demonstrated that including irrigation has a small yet robust beneficial effect on the representation of TXx and $T_{2m}$ in CESM over irrigated and all land pixels. By including CA, Hirsch et al. (2018) showed a general improvement in the simulation skill over MED for TXx and $T_{2m}$ and enhanced skill for $T_{2m}$ over WNA, CNA, and CEU.

### 2.3 Statistical analysis

The warming rate β was calculated using Sen's slope approach (Sen, 1968) based on the time and temperature values in each grid cell. This means that at each longitude and latitude point on land, there are 30 time measurements (1981-2010) with an

https://doi.org/10.5194/esd-2020-35
Preprint. Discussion started: 20 July 2020


Earth System Dynamics Discussions

associated temperature measurement (for each annual mean $T_{2m}$ and TXx). Therefore, there are 30x29/2 possible pairs of sample points, rendering 435 pairs for each location.

Annual TXx and $T_{2m}$ values averaged across all land pixels and all irrigated pixels were computed for the CTL, IRR and CA ensemble means, as well as the GHCNDEX (TXx), HadEX2 (TXx) and CRU ($T_{2m}$) observations. A Sen's slope regression analysis was then carried out on the spatial mean temperatures of TXx and $T_{2m}$ change over time (1981-2010) for (a) all pixels, (b) irrigated pixels and (c) CA pixels only, for both observations and the model ensembles.

The spatial mean warming rate across all (land or irrigated) pixels was also calculated. Additionally, all pixels within the SREX regions where irrigation is extensive (Thiery et al., 2017) –WNA, CNA, MED, WAS, SAS, SEA and EAS – were selected and their spatial means determined and examined. The SREX regions where CA is extensive (Hirsch et al., 2018) were also examined in greater detail. These include WNA, CNA, MED, SSA, CEU and SAU (Figure 1).

## 3 Results

### 3.1 Model Evaluation

This section explores how the existing CESM climate simulation skill (i.e. how well the simulated and observed trends agree) is altered in IRR and CA relative to the skill obtained in the CTL. The model biases and spatial root mean square error (RMSE) values relative to the warming trends of the $T_{2m}$ and TXx global observational products are provided in Table 1. The CTL ensemble underestimates the mean $T_{2m}$ warming trends by ~0.004 K $yr^{-1}$ over all land pixels and ~0.003 K $yr^{-1}$ over irrigated pixels. In contrast, for the IRR ensemble, $T_{2m}$ warming trends are overestimated by ~0.001 K $yr^{-1}$ across irrigated pixels, whereas over CA pixels $T_{2m}$ warming trends are overestimated by ~0.002-0.004 K $yr^{-1}$ in both the CA and CTL ensemble. On average, CESM also overestimates TXx warming trends by ~0.007–0.03 K $yr^{-1}$ over all land pixels in the three ensembles, ~0.008–0.013 K $yr^{-1}$ over irrigated pixels in the CTL and IRR ensembles and ~0.006–0.013 K $yr^{-1}$ over all CA pixels in the CTL and CA ensemble. This means that while $T_{2m}$ warming rates have a slight low bias on average over all land and partially over irrigated areas, TXx warming trends are consistently too high over all land, irrigated and CA areas.

To investigate how the uncertainty between the different irrigation and CA estimates of warming trends influences simulation skill, we examine the added value of including irrigation and CA for TXx and $T_{2m}$ over the regions where irrigation and/or the CA extent is greatest, as well as over global land, global irrigated land and global CA land (Figure 2). The added value is evaluated by calculating the change (experiment minus control) in the spatial RMSE. Accounting for irrigation improves the simulation skill for trends over MED, WAS and SAS for $T_{2m}$ and over MED, WAS, SAS and SEA

https://doi.org/10.5194/esd-2020-35
Preprint. Discussion started: 20 July 2020


Earth System Dynamics Discussions

for TXx (with HadEX2 as reference product). For WNA, CNA and EAS, the added value is negative or limited for both temperature metrics. Accounting for CA improves the simulation skill over CNA, CEU and SAU for the $T_{2m}$ and both TXx observational products and over the MED for the $T_{2m}$ and the TXx HaxEX2 observational products. For WNA, skill is reduced for all CA estimates. If we consider the grid cells where the land fraction within the CESM exceeds 50% ("all land") or just the grid cells that have a nonzero irrigation ("Irrigated land") is present, there is added value for $T_{2m}$ observational product over all land and the grid cells where irrigation has been applied. There is limited skill improvement for the TXx HadEx2 observational product. For the CA simulations, if we consider all land and the grid cells with a nonzero CA fraction ("CA land"), the model skill improves for the $T_{2m}$ observational product.

### 3.2 Impact of Irrigation and Conservation Agriculture on Mean and Extreme Warming Trends

Neither irrigation nor CA has a cooling effect on $T_{2m}$ warming rates in irrigated/CA or non-irrigated/CA regions (Figure 3a and 3c). Irrigation induced an increased $T_{2m}$ warming rate of 0.0023 K $yr^{-1}$ on average over land and 0.004 K $yr^{-1}$ across all irrigated pixels (Table 2). For context, the mean $T_{2m}$ CRU observed warming trend over irrigated pixels was 0.029 K $yr^{-1}$. As a result of CA, $T_{2m}$ warming rates increased by 0.002 K $yr^{-1}$ on average over land and 0.002 K $yr^{-1}$ across all CA pixels (Table 2). The mean $T_{2m}$ CRU observed warming trend over CA pixels was 0.024 K $yr^{-1}$.

Likewise, no cooling effect of irrigation or CA was evident on TXx warming rates in irrigated/CA or non-irrigated/CA regions, according to the warming rates generated (Figure 3b and 3d). Irrigation induced an increased TXx warming rate of 0.006 K $yr^{-1}$ on average over land and 0.004 K $yr^{-1}$ across all irrigated pixels (Table 2). The mean TXx observed warming trend over irrigated pixels was 0.022 K $yr^{-1}$ for HadEX2 and 0.025 K $yr^{-1}$ for GHCNDEX. Due to CA, TXx warming rates increased by 0.003 K $yr^{-1}$ on average over land and 0.005 K $yr^{-1}$ across all CA pixels (Table 2). The mean TXx observed warming trend over CA pixels was 0.033 K $yr^{-1}$ for HadEX2 and 0.031 K $yr^{-1}$ for GHCNDEX. The results suggest a slight irrigation- and CA-induced acceleration of the annual $T_{2m}$ and TXx warming trends, rather than the hypothesised cooling.

### 3.3 Spatial average

When the annual $T_{2m}$ and TXx temperatures are spatially averaged for each ensemble, the IRR and CTL simulations both overestimate observed values for irrigated pixels (Figure 4a and 4b), and the CA and CTL simulations both overestimate observed over CA pixels (Figure 4c and 4d). However, the impact of irrigation and CA on the modelled spatially averaged temperatures improves the closeness to that of the observations, i.e. there is an overall cooling-effect (Figure 4a-d), which is consistent with current theory (Kueppers et al., 2007; Saeed et al., 2009; Kueppers and Snyder, 2012; Thiery et al., 2017, 2020; Hirsch et al., 2018).

https://doi.org/10.5194/esd-2020-35
Preprint. Discussion started: 20 July 2020


Earth System Dynamics Discussions

What these results show in addition is, for the IRR and CA models – for all land, irrigated and CA pixels, the spatially averaged $T_{2m}$ and TXx warming rates are higher than those of the CTL model. Therefore, rather than continuous cooling, there is evidence in Figure 4 of a pulse cooling phase during the spin-up years (Smith et al., 1998), after which the $T_{2m}$ and TXx warming trends increases at a greater rate than the control simulations.

In the case of CA, the results indicate two opposing effects: (1) increased surface albedo associated with no tillage reduces the solar energy absorbed by the surface, inducing cooling (Davin et al., 2014); and (2) the presence of a crop residue over CA land can decrease soil evaporation, inhibiting energy partitioning to the latent heat flux, leading to surface warming (Hirsch et al., 2017). For TXx (Figure 4d), the second effect seems to dominate as the spatially averaged CA temperatures eventually surpass those of the CTL over CA pixels. This is likely because TXx is typically recorded during the summer/dry season – when crop residue is more likely to be applied to reduce evaporation, shifting the energy to the sensible heat flux and increasing TXx.

In the case of irrigation, the response also suggests two competing effects: (1) there is more water at the surface, so the energy budget shifts to the latent instead of sensible heat flux, resulting in evaporative cooling; and (2) because irrigation globally adds 418 $km^3$ $yr^{-1}$ of moisture to the atmosphere (Thiery et al., 2017) and as water vapour acts as a greenhouse gas it traps outgoing longwave radiation, radiating it back to the Earth's surface as downward longwave radiation, resulting in increased warming trends. The first effect appears more pronounced than the second due to the net cooling in Figure 4a and 4c. This means that despite the water vapour (acting as GHG) increases downward radiation and the overall energy budget thus increasing, most of it still goes to the latent heat flux leading to a net reduction in temperature (as compared to a situation without irrigation, where the sensible/latent ratio is more in favour of the latter). The limited warming effect of irrigation on atmospheric temperatures through water vapour forcing is consistent with earlier GCM studies inputting more than twice the amount of water vapour into the atmosphere through irrigation (32500 $m^3$ $s^{-1}$ or 1026 $km^3$ $yr^{-1}$) and finding limited radiative forcing (Boucher et al., 2004; Sherwood et al., 2018).

We further investigate the potential warming of the Earth System irrigation-induced enhanced atmospheric water vapour by computing the top-of-atmosphere net radiation ($R_{n,TOA}$) in the CTL and IRR ensembles over the 1981-2010 period (Figure 5). As both ensembles employ prescribed, transient sea surface temperatures, the difference in $R_{n,TOA}$ is a measure of irrigation-induced radiative forcing. The area-weighted global average $R_{n,TOA}$ is 0.4961 W $m^{-2}$ for the CTL ensemble (Figure 5a) and 0.5450 W $m^{-2}$ for the IRR ensemble (Figure 5b). The radiative forcing from irrigation is therefore 0.0489 W $m^{-2}$, at least an order of magnitude smaller compared to other combined anthropogenic forcings over this period (IPCC, 2013) and consistent with previous estimates (Boucher et al., 2004; Sherwood et al., 2018). The positive radiative forcing is mainly located over South Asia, and partially offset by negative forcing over central Asia, Greenland and Antarctica (Figure 5c). Breakdown of the irrigation-induced $R_{n,TOA}$ change into the shortwave and longwave components shows that the forcing is

https://doi.org/10.5194/esd-2020-35
Preprint. Discussion started: 20 July 2020


Earth System Dynamics Discussions

dominated by the longwave signal (+0.0583 W $m^{-2}$), with the shortwave signal even showing signs of a slight albedo increase (-0.0094 W $m^{-2}$), presumably from enhanced low-level cloud cover (Sherwood et al., 2018). The additional water vapor in the atmosphere and associated longwave trapping in CESM can thus explain the small, positive radiative forcing contributing to Earth System warming and associated enhanced near-surface temperature trends in irrigated regions (Figure 4a-b), but at the land surface this signal is too weak to offset the local pulse cooling from the irrigation-induced increase in evaporative fraction.

### 3.4 Subgrid-Scale Impacts

To examine heterogeneous influences within grid cells, subgrid tiles that represent local physical, biogeochemical, and ecological characteristics – and therefore local (subgrid) influences of irrigation and CA – were evaluated against regional (grid-scale) influences. Up to 21 surface tiles may occur within one grid cell in CLM4, including glacier, wetland, lake, urban, bare soil and 16 PFTs.

For subgrid irrigation influences (Figure 6a and 6c), all tiles are placed on one single soil column, except for the irrigated crop tile. Separating the soil columns in this way allows the soils underneath irrigated and rainfed crop tiles to have individual responses to atmospheric forcing (Schultz et al., 2016). Therefore, the subgrid-scale difference is the irrigated crop tile ($IRR_{SUB}$ in Table 2) minus the rainfed crop tile (RAIN in Table 2). For subgrid CA influences (Figure 6b and 6d), using the PFT-level outputs from CLM it is possible to examine the subgrid-scale differences between the CA crop tiles ($CA_{SUB}$ in Table 2) and conventionally managed crop tiles (CM in Table 2), thus $CA_{SUB}$ minus CM represents the subgrid-scale effect.

Our results indicate a subgrid-scale cooling effect of irrigation on surface radiative temperature ($T_S$) warming trends that is more distinct and spatially consistent over irrigated pixels than grid-scale effects (Figures 6a and 6c). $T_S$ warming trends on irrigated tiles are on average -0.008 K $yr^{-1}$ (-24%) lower than their rainfed counterparts, whereas the trends are on average 0.001 K $yr^{-1}$ (+11%) higher on the grid cell level over irrigated land (Table 2). The subgrid-scale influences of irrigation on ET rates over irrigated tiles were also pronounced as they increased by 0.653 mm $yr^{-1}$ in comparison to rainfed tiles (Figure 6e and Table 2).

The subgrid-scale influences of CA on $T_S$ warming trends are smaller in comparison to irrigation, with only a 0.001 K $yr^{-1}$ (-3%) dampening of warming trends and ET rates increased by 0.083 mm $yr^{-1}$ (46%), relative to their conventionally managed counterparts (Figure 6b and 6d and Table 2).

https://doi.org/10.5194/esd-2020-35
Preprint. Discussion started: 20 July 2020


Earth System Dynamics Discussions

The cooler warming trends from irrigation at the subgrid-scale (Figure 6a) occurs where the ET rate increases (Figure 6g), suggesting the cooling is due to an increase in the latent heat flux, which is consistent with Cook et al. (2015) and Thiery et al. (2017). The heightened grid-scale $T_S$ warming trends (Figure 6c) generally align with a greater total atmospheric column water (TMQ) flux (Figure 6e) and increased $T_{2m}$ warming trends over irrigated pixels (Figure 4a and 3a), which signifies the longwave radiation trapping potential of the additional atmospheric water vapour. As the impact on trends is small (e.g. $T_{2m}$ and $T_s$ warming trends increased, respectively, by 0.004 K $yr^{-1}$ and 0.001 K $yr^{-1}$ across irrigated pixels), the finding is in agreement with Sherwood et al. (2018) who showed that additional water vapour has a small impact on global warming potential mainly because it rains out before reaching the altitudes needed to significantly contribute to the greenhouse effect. These findings thus support the concept of radiative forcing and the proviso that, at the land surface, the water vapour signal does not offset local cooling from the irrigation-induced increase in evaporative fraction, as described for Figure 4 and 5 and previously proposed by Boucher et al. (2004). However, because the subgrid-scale $T_s$ trends, in contrast to grid-scale trends, are computed within the same ensemble and thus do not account for atmospheric (water vapour) feedbacks, the sign reversal of irrigation-induced impact on grid-scale and subgrid-scale $T_s$ trends confirms the importance of atmospheric feedbacks (water vapour forcing) in explaining the increased grid-scale $T_s$ and $T_{2m}$ trends.

When spatially averaged, over all pixels, the $T_S$ warming trends at the subgrid-scale show no evidence of a pulse cooling phase due to irrigation (Figure 7c), which is in contrast the results over irrigated pixels – where there is both a cooling effect on $T_S$ and a dampening of $T_S$ warming trends (Figure 7a). This contrast is likely due to a combination of the remote effects of irrigation, the larger contribution of natural variability and an increased relative contribution of other components when considering all land pixels (Puma and Cook, 2010; Cook et al., 2015; De Vrese et al., 2016; Thiery et al., 2017).

Regarding CA, the slight overall warming of $T_S$ temperatures is possibly because of the decrease in soil evaporation as a result of crop residue over CA land (Figure 7b), inhibiting energy partitioning to the latent heat flux. Over all land pixels (Figure 7d), however, the subgrid-scale response suggests that the effect of increasing surface albedo and thus reducing the solar energy absorbed by the surface is dominant. Additionally, the close correspondence between CA and CM (Figure 7b) may reflect that the temperature response spatially is both positive and negative depending on which mechanism dominates and therefore the spatial aggregation for all CA and all CM pixels globally looses this (Figure 7d).

## 4 Discussion

This study examined the hypothesis of whether excluding a theoretical constant level of irrigation and CA contributes to the overestimation of warming by an Earth System Model. A Sen's slope model was built and applied to ensemble simulations from the Community Earth System Model that include irrigation parameterization to determine if there are spatiotemporal

https://doi.org/10.5194/esd-2020-35
Preprint. Discussion started: 20 July 2020


patterns and why they exist. This unexpectedly showed that warming trends are not dampened due to irrigation and CA, except for the subgrid-scale effect of irrigation on the warming trends of $T_S$.

The key findings of this investigation are a net cooling effect of irrigation and CA on the modelled spatially averaged $T_{2m}$ and TXx, but, rather than continuous cooling, the warming trends showed a pulse cooling phase, after which the sensitivity to climatic change remains. Under irrigation, the opposing effects are the result of: (1) evaporative cooling; and (2) atmospheric water vapour strengthening the greenhouse effect. Under CA, the contrasting effects are due to: (1) cooling from a tillage-induced increase in surface albedo; and (2) reduced soil evaporation due to the presence of crop residue, limiting energy partitioning to the latent heat flux. At the subgrid-scale, there was both a cooling effect on $T_S$ and in the dampening of warming trends. This implies that enhanced evaporative cooling is the dominant driver of the subgrid-scale temperature trends.

Although this study was constructed with great care and built on a state-of-the-art modelling suite, several future developments could improve understanding of the impact of irrigation and CA on climate. Firstly, the quality of the model(s) could be improved by using transient irrigation and CA extents and new land cover datasets from the 6$^{th}$ phase of the Coupled Model Intercomparison Project (CMIP6) (Lawrence et al., 2016). In this study, a static irrigation map for the year 2000 was used for the whole simulation period. This likely contributes to our results being conservative. If, for instance, irrigation expands over time, the cooling effect may become stronger and thus affect the warming trends. Also, CMIP6 experiments are based on annual emissions, whereas CMIP5 was based on decadal emissions and CMIP6 models were updated with irrigation-related features and land cover maps that incorporate irrigation and CA expansion over time (Goddard et al., 2013; Miao et al., 2014; Boer et al., 2016; Meinshausen et al., 2017; Stouffer et al., 2017). CMIP6 models may therefore improve the dynamics between irrigation, CA and climate change, provided that they represent these land management techniques in their surface schemes.

The second consideration is that all simulations used in this study (5 control, 5 irrigation and 5 CA) were from a single model. Ensembles completed as such with the same model but different simulations (i.e. based on different initial conditions) characterise the uncertainty associated with internal climate variability only, while multi-model ensembles also account for the impact of model differences (Tebaldi and Knutti, 2007; Knutti et al., 2010). Therefore, this study should ideally be repeated with other models. Donat et al. (2017) conducted their study on 20 CMIP5 models, but these models did not incorporate irrigation and CA.

Thirdly, irrigation and CA are the only agricultural management practices considered in this study (and done so individually), whereas other agricultural management practices have been shown as impactful (Luyssaert et al., 2014; Erb et al., 2016, 2018). Trend analysis of integrated land management practices could affect the outcome if there is a lumped effect.

https://doi.org/10.5194/esd-2020-35
Preprint. Discussion started: 20 July 2020


Earth System Dynamics Discussions

Building an additional stochastic model could account for variations in the distribution of the impact of land management practices on warming trends. This would enable sensitivity analyses to ascertain the relative importance of irrigation and CA to the total warming trends (based on all land management practices), as well as the relative contributions of the uncertainty sources (model input, parameter, structure) to the total uncertainty in the model output.

The final consideration is whether regression-based models are suitable for analysing changes in highly variable climate data, particularly annual extreme temperature data (von Storch, 2006). Essentially, the regression slope blends forced temperature change and variability, to provide an estimation of the temperature variation over time – within which variance can be lost due to noisy data. Whether the TXx and $T_{2m}$ temperatures were first spatially averaged and then the slope retrieved or if each slope was estimated for each gridcell and then the overall trends examined, the outcome remains. This is unsurprising considering that in the spatial averaging the noise contributions are averaged out, while the individual regression data suffers from the variance loss related to regression. However, when applied to over 60 years of observational data, the regression model used in this study showed similar trends to using the difference between the past and the present average temperatures (not shown). This implies that the irrigation and CA-inclusive climate system may require a longer timeframe (than the 30 years plus a 5-year spin-up period used) for trends to overtake the natural variability. Additionally, rather than aggregating all months, trends during individual months or seasons could be examined. This can affect, for instance, the influence of irrigation on $T_s$, which has a clear seasonal pattern, with more cooling during the driest and/or hottest months (Thiery et al., 2017). A smaller magnitude in TXx response to CA at the subgrid-scale has also been noted during the summer season due to a larger leaf area index reducing soil surface exposure and thus the contrast between CA and conventionally managed crops (Hirsch et al., 2018).

## 5 Conclusion

In this study the impact of a theoretical constant level of irrigation and CA on warming trends in global climate and climate extremes was assessed for the period of 1981–2010 using the Community Earth System Model. A Sen's slope regression-based analysis was performed to compute spatial-explicit warming trends and spatially averaged warming trends. Insight into how modelled temperature is affected in its median by irrigation and CA over time was provided.

An irrigation- and CA-induced acceleration of the annual $T_{2m}$ and TXx warming trends was evident. Estimating the impact of irrigation and CA on the spatial average of the warming trends indicated that irrigation and CA have a pulse cooling effect on $T_{2m}$ and TXx, after which warming trends increased at a greater rate than the control simulations. This differed at the subgrid-scale under irrigation where surface temperature cooling and the dampening of warming trends were both evident. Therefore, irrigation-induced evaporative cooling is a more dominant effect at the local level than the strengthening of the greenhouse effect at regional scales as a result of enhanced atmospheric water vapour.

https://doi.org/10.5194/esd-2020-35
Preprint. Discussion started: 20 July 2020


Earth System Dynamics Discussions

A model evaluation demonstrated that the simulations accounting for irrigation and CA satisfactorily reproduce observed warming trends in $T_{2m}$, but not the trends in temperature extremes of TXx. This signifies that the GCMs have more trouble representing the greater variability in the extreme temperatures, compared to that of the mean annual temperature, and that the Sen's slope models are more suited to the blended variability inherent to annual mean temperatures.

The findings overall emphasise the need for a more in-depth evaluation of the sensitivity of future climate projections to irrigation and CA-induced temperature changes. A sensitivity analysis, using transient irrigation and CA extents, as well as additional land management techniques and climate models based on CMIP6 output, is recommended. In this way, the variance can be approximated and the relative contributions of the uncertainty sources to the total uncertainty in the model output, as well as the relative importance of irrigation and CA to the total warming trends, can be quantified and compared. If the fundamental uncertainties relating to model structure dominate, then a model more detailed analysis than the regression approach used in this study is suggested. This will support decision-making when planning land management strategies that combine resource use efficiency with climate change adaptation and mitigation, enabling sustainable intensification of land management to meet mitigation targets and future demand for food, fuel, fibre, and water.

## Acknowledgments

We thank Prof Piers Forster and Dr Chris Smith at the University of Leeds for their valuable discussions and insight on the theoretical outcomes of this project.

L. Hirsch is supported through funding from the Australian Research Council (ARC) Centre of Excellence for Climate Extremes (CE170100023).

## References

Boer, G. J., Smith, D. M., Cassou, C., Doblas-Reyes, F., Danabasoglu, G., Kirtman, B., Kushnir, Y., Kimoto, M., Meehl, G. A., Msadek, R., Mueller, W. A., Taylor, K. E., Zwiers, F., Rixen, M., Ruprich-Robert, Y., and Eade, R.: The Decadal Climate Prediction Project (DCPP) contribution to CMIP6, Geoscientific Model Development, doi: 10.5194/gmd-9-3751-2016, 2016.

Boucher, O., Myhre, G., and Myhre, A.: Direct human influence of irrigation on atmospheric water vapour and climate, Climate Dynamics, doi: 10.1007/s00382-004-0402-4, 2004.

Carrer, D., Pique, G., Ferlicoq, M., Ceamanos, X., and Ceschia, E.: What is the potential of cropland albedo management in the fight against global warming? A case study based on the use of cover crops, Environmental Research Letters, 13 044030, doi: 10.1088/1748-9326/aab650, 2018.

https://doi.org/10.5194/esd-2020-35
Preprint. Discussion started: 20 July 2020


Cook, B. I., Shukla, S. P., Puma, M. J., and Nazarenko, L. S.: Irrigation as an historical climate forcing, Climate Dynamics, doi: 0.1007/s00382-014-2204-7, 2015.

Davin, E. L., Seneviratne, S. I., Ciais, P., Olioso, A., and Wang, T.: Preferential cooling of hot extremes from cropland albedo management, Proceedings of the National Academy of Sciences, doi: 10.1073/pnas.1317323111, 2014.

De Vrese, P., Hagemann, S., and Claussen, M.: Asian irrigation, African rain: Remote impacts of irrigation, Geophysical Research Letters, doi: 10.1002/2016GL068146, 2016.

Donat, M. G., Alexander, L. V., Yang, H., Durre, I., Vose, R., and Caesar, J.: Global Land-Based Datasets for Monitoring Climatic Extremes, Bulletin of the American Meteorological Society, doi: 10.1175/BAMS-D-12-00109.1, 2013a.

Donat, M. G., Alexander, L. V., Yang, H., Durre, I., Vose, R., Dunn, R. J. H., Willett, K. M., Aguilar, E., Brunet, M., Caesar, J., Hewitson, B., Jack, C., Klein Tank, A. M. G., Kruger, A. C., Marengo, J., Peterson, T. C., Renom, M., Oria Rojas, C., Rusticucci, M., Salinger, J., Elrayah, A. S., Sekele, S. S., Srivastava, A. K., Trewin, B., Villarroel, C., Vincent, L. A., Zhai, P., Zhang, X., and Kitching, S.: Updated analyses of temperature and precipitation extreme indices since the beginning of the twentieth century: The HadEX2 dataset, Journal of Geophysical Research Atmospheres, doi: 10.1002/jgrd.50150, 2013b.

Donat, M. G., Pitman, A. J., and Seneviratne, S. I.: Regional warming of hot extremes accelerated by surface energy fluxes, Geophysical Research Letters, doi: 10.1002/2017GL073733, 2017.

Erb, K. H., Fetzel, T., Plutzar, C., Kastner ,T., Lauk, C., Mayer, A., Niedertscheider, M., Körner, C., and Haberl, H.: Biomass turnover time in terrestrial ecosystems halved by land use, Nature Geoscience, doi: 0.1038/ngeo2782, 2016.

Erb, K. H., Kastner, T., Plutzar, C., Bais, A. L. S., Carvalhais, N., Fetzel, T., Gingrich, S., Haberl, H., Lauk, C., Niedertscheider, M., Pongratz, J., Thurner, M., and Luyssaert, S.: Unexpectedly large impact of forest management and grazing on global vegetation biomass, Nature, doi: 10.1038/nature25138, 2018.

Fereres, E., and Connor, D.: Sustainable water management in agriculture, Challenges of the New Water Policies for the XXI Century: Proceedings of the Seminar on Challenges of the New Water Policies for the 21st Century, 2004.

Fereres, E., and Soriano, M. A.: Deficit irrigation for reducing agricultural water use, Journal of Experimental Botany, 58, 147-159, 2007.

Fischer, E. M., and Knutti, R.: Anthropogenic contribution to global occurrence of heavy-precipitation and high-temperature extremes, Nature Climate Change, doi: 10.1038/nclimate2617, 2015.

Goddard, L., Kumar, A., Solomon, A., Smith, D., Boer, G., Gonzalez, P., Kharin, V., Merryfield, W., Deser, C., Mason, S. J., Kirtman, B. P., Msadek, R., Sutton, R., Hawkins, E., Fricker, T., Hegerl, G., Ferro, C. A. T., Stephenson, D. B., Meehl, G. A., Stockdale, T., Burgman, R., Greene, A. M., Kushnir, Y., Newman, M., Carton, J., Fukumori, I., and Delworth, T.: A verification framework for interannual-to-decadal predictions experiments, Climate Dynamics, doi: 10.1007/s00382-012-1481-2, 2013.

Harris, I., Jones, P. D., Osborn, T. J., and Lister, D.H.: Updated high-resolution grids of monthly climatic observations - the CRU TS3.10 Dataset, International Journal of Climatology, doi: 10.1002/joc.3711, 2014.

https://doi.org/10.5194/esd-2020-35
Preprint. Discussion started: 20 July 2020


Hartmann, D. L., Tank, A. M. G. K., Rusticucci, M., Alexander, L., Brönnimann, S., Charabi, Y., Dentener, F., Dlugokencky, E., Easterling, D., Kaplan, A., Soden, B., Thorne, P., Wild, M., and Zhai, P. M.: Observations: Atmosphere and Surface Supplementary Material, Climate Change 2013 the Physical Science Basis: Working Group I Contribution to the Fifth Assessment Report of the Intergovernmental Panel on Climate Change, 2013.

Hauser, M., Thiery, W., and Seneviratne, S. I: Potential of global land water recycling to mitigate local temperature extremes, Earth System Dynamics, doi:10.5194/esd-10-157-2019, 2019.

Hirsch, A. L., Prestele, R., Davin, E. L., Seneviratne, S. I., Thiery, W., and Verburg, P. H.: Modelled biophysical impacts of conservation agriculture on local climates, Global Change Biology, doi:10.1111/gcb.14362, 2018.

Hirsch, A. L., Wilhelm, M., Davin, E. L., Thiery, W., and Seneviratne, S. I.: Can climate-effective land management reduce regional warming? Journal of Geophysical Research, doi: 10.1002/2016JD026125, 2017.

Hurrell, J. W., Holland, M. M., Gent, P. R., Ghan, S., Kay, J. E., Kushner, P. J., Lamarque, J. F., Large, W. G., Lawrence, D., Lindsay, K., Lipscomb, W. H., Long, M. C., Mahowald, N., Marsh, D. R., Neale, R. B., Rasch, P., Vavrus, S., Vertenstein, M., Bader, D., Collins, W. D., Hack, J. J., Kiehl, J., and Marshall, S.: The community earth system model: A framework for collaborative research, Bulletin of the American Meteorological Society, doi: 10.1175/BAMS-D-12-00121.1, 2013.

IPCC.: Summary for policymakers. Climate Change 2014: Impacts, Adaptation, and Vulnerability. Part A: Global and Sectoral Aspects. Contribution of Working Group II to the Fifth Assessment Report of the Intergovernmental Panel on Climate Change, 2013.

Jia, G., Shevliakova, E., Artaxo, P., De Noblet-Ducoudré, N., Houghton, R., House, J., Kitajima, K., Lennard, C., Popp, A., Sirin, A., Sukumar, R., and Verchot, L.: Land–climate interactions. In: Climate Change and Land: an IPCC special report on climate change, desertification, land degradation, sustainable land management, food security, and greenhouse gas fluxes in terrestrial ecosystems [P.R. Shukla, J. Skea, E. Calvo Buendia, V. Masson-Delmotte, H.-O. Pörtner, D.C. Roberts, P. Zhai, R. Slade, S. Connors, R. van Diemen, M. Ferrat, E. Haughey, S. Luz, S. Neogi, M. Pathak, J. Petzold, J. Portugal Pereira, P. Vyas, E. Huntley, K. Kissick, M, Belkacemi, J. Malley, (eds.)], 2019.

Jones, P. W.: First- and second-order conservative remapping schemes for grids in spherical coordinates, Monthly Weather Review, doi: 10.1175/1520-0493(1999)127<2204:FASOCR>2.0.CO;2, 1999.

Kassam, A., Friedrich, T., Derpsch, R., and Kienzle, J.: Overview of the worldwide spread of conservation agriculture, Field Actions Science Report, 2015.

Knutti, R., Furrer, R., Tebaldi, C., Cermak, J., and Meehl, G.A.: Challenges in combining projections from multiple climate models, Journal of Climate, doi: 10.1175/2009JCLI3361.1, 2010.

Kueppers, L. M., and Snyder, M. A.: Influence of irrigated agriculture on diurnal surface energy and water fluxes, surface climate, and atmospheric circulation in California, Climate Dynamics, doi: 10.1007/s00382-011-1123-0, 2012.

Kueppers, L. M., Snyder, M. A., and Sloan, L. C.: Irrigation cooling effect: Regional climate forcing by land-use change, Geophysical Research Letters, doi: 10.1029/2006GL028679, 2007.


Lawrence, D. M., Hurtt, G. C., Arneth, A., Brovkin, V., Calvin, K. V., Jones, A. D., Jones, C. D., Lawrence, P. J., Noblet-Ducoudré, N. De., Pongratz, J., Seneviratne, S. I., and Shevliakova, E.: The Land Use Model Intercomparison Project (LUMIP) contribution to CMIP6: Rationale and experimental design, Geoscientific Model Development, doi: 10.5194/gmd-9-2973-2016, 2016.

Lombardozzi, D. L., Bonan, G. B., Wieder, W., Grandy, A. S., Morris, C., and Lawrence, D. L.: Cover crops may cause winter warming in snow-covered regions, Geophysical Research Letters, doi: 10.1029/2018GL079000, 2018.

Luyssaert, S., Jammet, M., Stoy, P. C., Estel, S., Pongratz, J., Ceschia, E., Churkina, G., Don, A., Erb, K., Ferlicoq, M., Gielen, B., Grünwald, T., Houghton, R. A., Klumpp, K., Knohl, A., Kolb, T., Kuemmerle, T., Laurila, T., Lohila, A., Loustau, D., McGrath, M. J., Meyfroidt, P., Moors, E. J., Naudts, K., Novick, K., Otto, J., Pilegaard, K., Pio, C. A., Rambal, S., Rebmann, C., Ryder, J., Suyker, A. E., Varlagin, A., Wattenbach, M., and Dolman, A.J.: Land management and land-cover change have impacts of similar magnitude on surface temperature, Nature Climate Change, doi: 10.1038/nclimate2196, 2014.

Meinshausen, M., Vogel, E., Nauels, A., Lorbacher, K., Meinshausen, N., Etheridge, D. M., Fraser, P. J., Montzka, S. A., Rayner, P. J., Trudinger, C. M., Krummel, P. B., Beyerle, U,. Canadell, J. G., Daniel, J. S., Enting, I. G., Law, R. M., Lunder, C. R,. O'Doherty, S., Prinn, R. G., Reimann, S., Rubino, M., Velders, G. J. M., Vollmer, M. K., Wang, R. H. J., and Weiss, R.: Historical greenhouse gas concentrations for climate modelling (CMIP6), Geoscientific Model Development, doi: 10.5194/gmd-10-2057-2017, 2017.

Miao, C., Duan, Q., Sun, Q., Huang, Y., Kong, D., Yang, T., Ye, A., Di, Z., and Gong, W.: Assessment of CMIP5 climate models and projected temperature changes over Northern Eurasia, Environmental Research Letters, doi: 10.1088/1748-9326/9/5/055007, 2014.

Oleson, K. W., Lawrence, D. M., Gordon, B., Flanner, M. G., Kluzek, E., Peter, J., Levis, S., Swenson, S. C., Thornton, E., and Feddema, J.: Technical description of version 4.0 of the Community Land Model (CLM), NCAR/TN-503+STR NCAR Technical Note, 2013.

Pendergrass, A. G., and Hartmann, D. L.: Changes in the distribution of rain frequency and intensity in response to global warming, Journal of Climate, doi: 10.1175/JCLI-D-14-00183.1, 2014.

Prestele, R., Hirsch, A. L., Davin, E. L., Seneviratne, S. I., and Verburg, P.H.: A spatially explicit representation of conservation agriculture for application in global change studies, Global Change Biology, doi: 10.1111/gcb.14307, 2018.

Puma, M. J. and Cook, B. I.: Effects of irrigation on global climate during the 20th century, Journal of Geophysical Research Atmospheres, doi: 10.1029/2010JD014122, 2010.

Saeed, F., Hagemann, S., and Jacob, D.: Impact of irrigation on the South Asian summer monsoon, Geophysical Research Letters, doi: 10.1029/2009GL040625, 2009.

Schultz, N. M., Lee, X., Lawrence, P. J., Lawrence, D. M., and Zhao, L.: Assessing the use of subgrid land model output to study impacts of land cover change, Journal of Geophysical Research, doi: 10.1002/2016JD025094, 2016.

Sen, P. K.: Estimates of the Regression Coefficient Based on Kendall's Tau, Journal of the American Statistical Association,


doi: 10.1080/01621459.1968.10480934, 1968.

Seneviratne, S. I., Corti, T., Davin, E. L., Hirschi, M., Jaeger, E. B., Lehner, I., Orlowsky, B., and Teuling, A. J.: Investigating soil moisture-climate interactions in a changing climate: A review, Earth-Science Reviews, 2010.

Seneviratne, S. I., Wilhelm, M., Stanelle, T., Van Den Hurk, B., Hagemann, S., Berg, A., Cheruy, F., Higgins, M. E., Meier, A., Brovkin, V., Claussen, M., Ducharne, A., Dufresne, J. L., Findell, K. L., Ghattas, J., Lawrence, D. M., Malyshev, S., Rummukainen, M., and Smith, B.: Impact of soil moisture-climate feedbacks on CMIP5 projections: First results from the GLACE-CMIP5 experiment, Geophysical Research Letters, doi: 10.1002/grl.50956, 2013.

Sherwood, J., Clabeaux, R., and Carbajales-Dale, M.: An extended environmental input-output lifecycle assessment model to study the urban food-energy-water nexus, Environmental Research Letters, doi: 10.1088/1748-9326/aa83f0, 2017.

Sherwood, S. C., Dixit, V., and Salomez, C.: The global warming potential of near-surface emitted water vapour, Environmental Research Letters, doi: 10.1088/1748-9326/aae018, 2018.

Siebert, S., Döll, P., Hoogeveen, J., Faures, J. M., Frenken, K., and Feick, S.: Development and validation of the global map of irrigation areas, Hydrology and Earth System Sciences, doi: 10.5194/hess-9-535-2005, 2005.

Sillmann, J., and Croci-Maspoli, M.: Present and future atmospheric blocking and its impact on European mean and extreme climate, Geophysical Research Letters, doi: 10.1029/2009GL038259, 2009.

Smith, R. A., Ditmire, T., and Tisch, J. W. G.: Characterization of a cryogenically cooled high-pressure gas jet for laser/cluster interaction experiments, Review of Scientific Instruments, doi: 10.1063/1.1149181, 1998.

Stouffer, R. J., Eyring, V., Meehl, G. A., Bony, S., Senior, C., Stevens, B., and Taylor, K. E.: CMIP5 scientific gaps and recommendations for CMIP6, Bulletin of the American Meteorological Society, doi: 10.1175/BAMS-D-15-00013.1, 2017.

Tebaldi, C., and Knutti, R.: The use of the multi-model ensemble in probabilistic climate projections, Philosophical Transactions of the Royal Society A: Mathematical, Physical and Engineering Sciences, 2007.

Thiery, W., Davin, E. L., Lawrence, D. M., Hirsch, A. L., Hauser, M., and Seneviratne, S. I.: Present-day irrigation mitigates heat extremes, Journal of Geophysical Research, doi: 10.1002/2016JD025740, 2017.

Thiery, W., Visser, A. J., Fischer, E. M., Hauser, M., Hirsch, A. L., Lawrence, D. M., Lejeune, Q., Davin, E. L., and Seneviratne, S. I.: Warming of hot extremes alleviated by expanding irrigation, Nature Communications, doi: 10.1038/s41467-019-14075-4, 2020.

Vogel, M. M., Orth, R., Cheruy, F., Hagemann, S., Lorenz, R., van den Hurk, B. J. J. M., and Seneviratne, S. I.: Regional amplification of projected changes in extreme temperatures strongly controlled by soil moisture-temperature feedbacks, Geophysical Research Letters, doi:10.1002/2016GL071235, 2017.

Vogel, M. M., Zscheischler, J., & Seneviratne, S. I.: Varying soil moisture-atmosphere feedbacks explain divergent temperature extremes and precipitation projections in central Europe. Earth System Dynamics, doi: 10.5194/esd-9-1107-2018, 2018.

von Storch H.: Response to Comment on “Reconstructing Past Climate from Noisy Data”, Science, doi:

https://doi.org/10.5194/esd-2020-35
Preprint. Discussion started: 20 July 2020


Earth System Dynamics
Discussions
Open Access
EGU

10.1126/science.1121571, 2006.

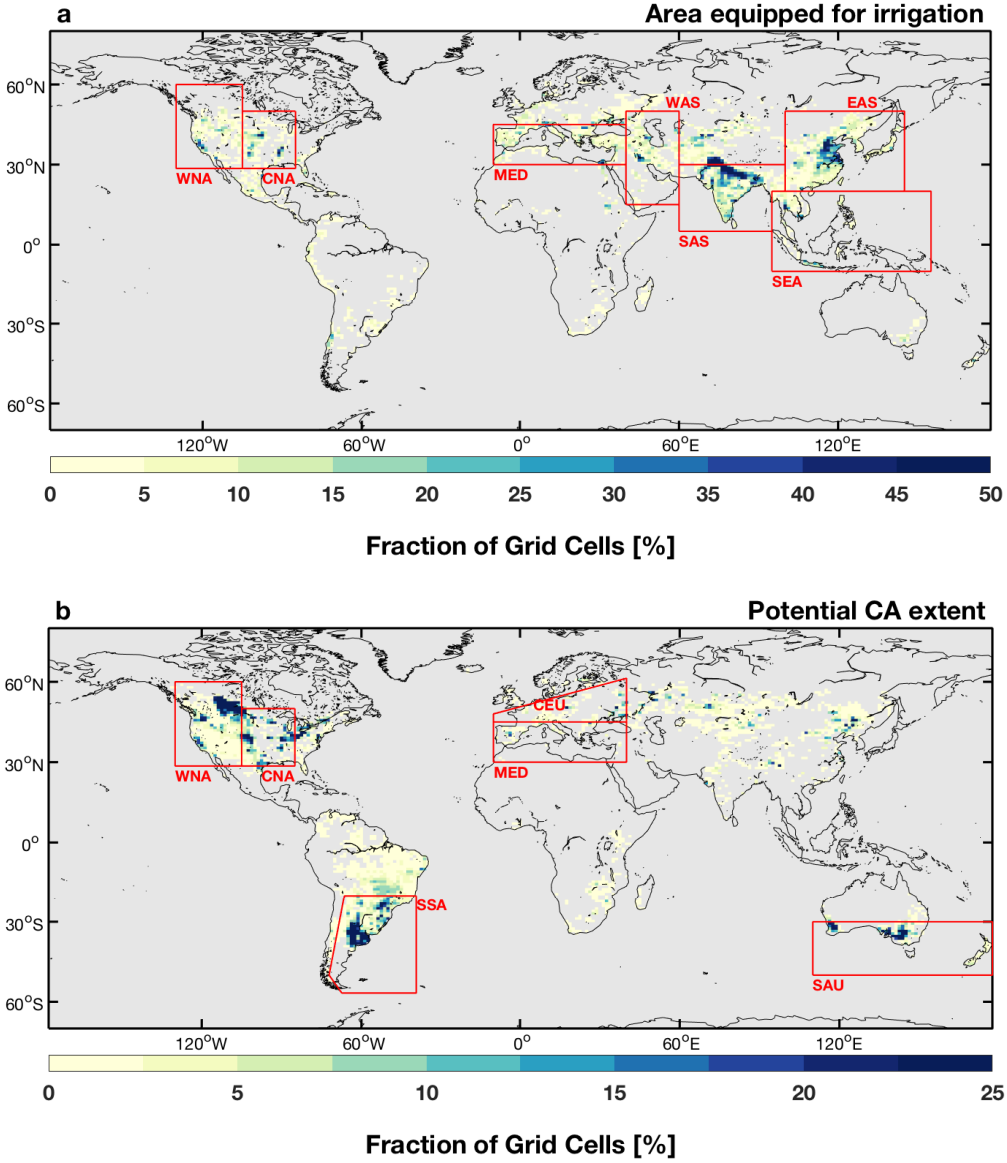


555

**Figure 1. (a) Percentage of each grid cell equipped for irrigation (%) (Siebert *et al.*, 2005). (b) Potential estimate of CA extent mapped to the CLM crop PFT (Prestele *et al.*, 2018). The red boxes in (a) denote the regional domains examined in greater detail including Western North America (WNA), Central North America (CNA), south Europe and Mediterranean (MED), West Asia**
560 **(WAS), South Asia (SAS), Southeast Asia (SEA), and East Asia (EAS). The red boxes in (b) denote the regional domains examined in greater detail including WNA, CNA, MED, South-eastern South America (SSA), Central Europe (CEU) and Southern Australia (SAU).**

https://doi.org/10.5194/esd-2020-35
Preprint. Discussion started: 20 July 2020


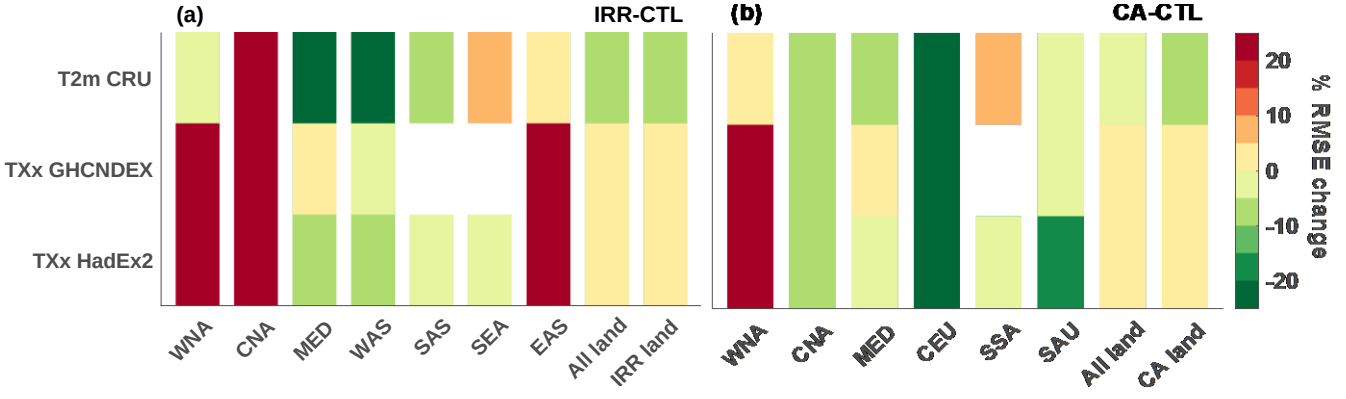


**Figure 2. Added value of including irrigation and CA in the simulated warming trends over 1981-2010. Percentage change in spatial root-mean-square error (RMSE) for the (a) IRR and (b) CA ensemble relative to the CTL ensemble over different regions (x axis) and with respect to 3 observational products (y axis). Considered regions are the SREX regions highlighted in Figure 1, in addition to global land, global irrigated land and global CA land. Observational products are for near-surface air temperature $T_{2m}$ (CRU), annual maximum daytime temperature TXx (GHCNDEX and HadEX2). The spatial RMSEs are computed for the ensemble mean warming trend in every pixel, and subsequently averaged over the selected region. Regions with an observational coverage below 50% are marked in white.**

https://doi.org/10.5194/esd-2020-35
Preprint. Discussion started: 20 July 2020


Earth System Dynamics
Discussions
Open Access
EGU

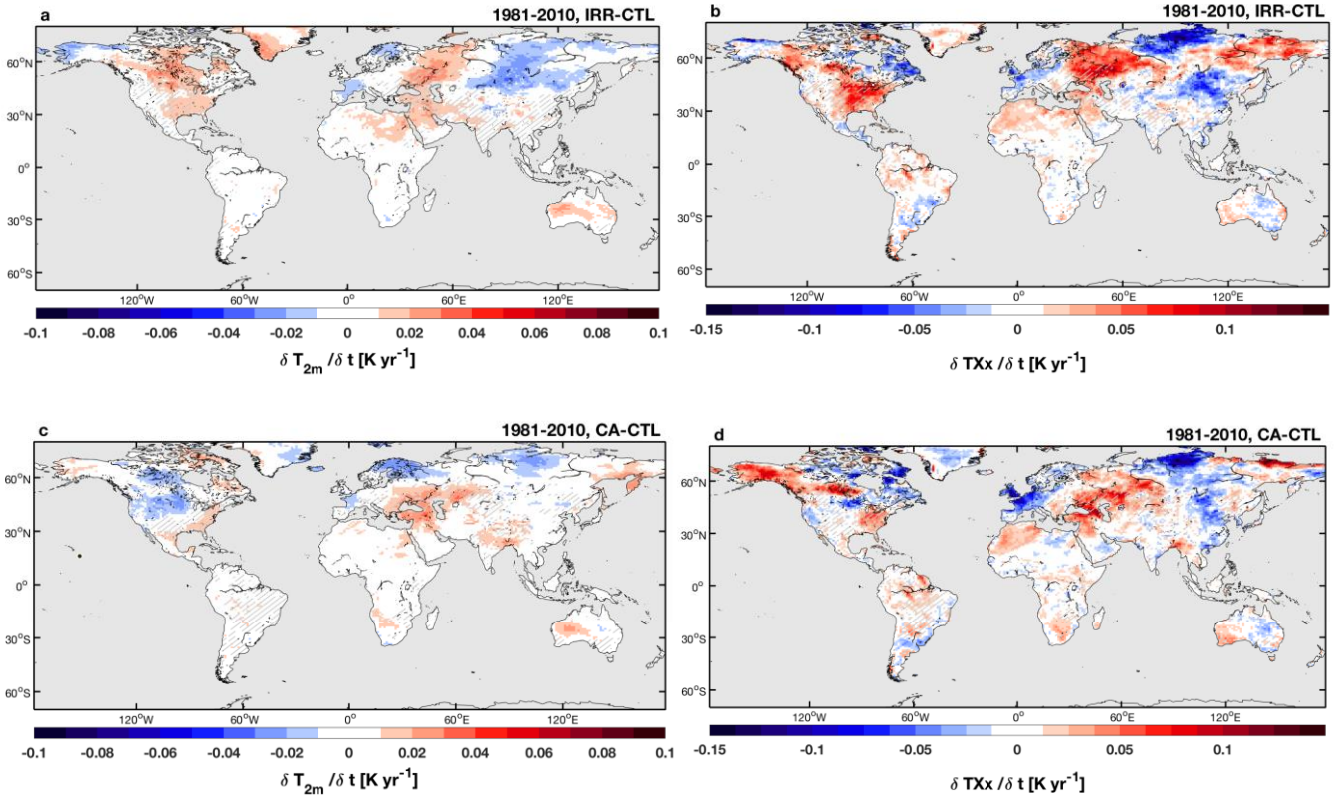


575

**Figure 3. Impact of irrigation (IRR minus control) on the warming trends of (a) near-surface air temperature ($T_{2m}$) and (b) maximum daytime temperature (TXx). Impact of conservation agriculture (CA minus control) on (a) $T_{2m}$ and (d) TXx warming trends. Hatching denotes less than 10% change induced by the model on mean warming trends of the lumped ensemble members.**

580

https://doi.org/10.5194/esd-2020-35
Preprint. Discussion started: 20 July 2020


Earth System Dynamics
Discussions
Open Access
EGU

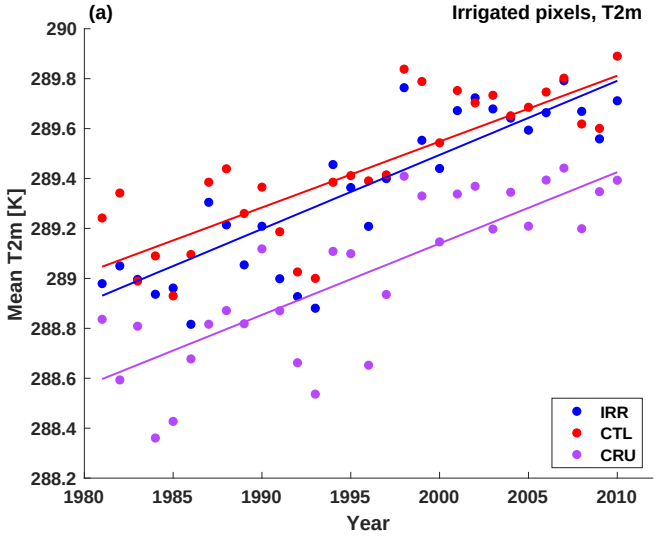


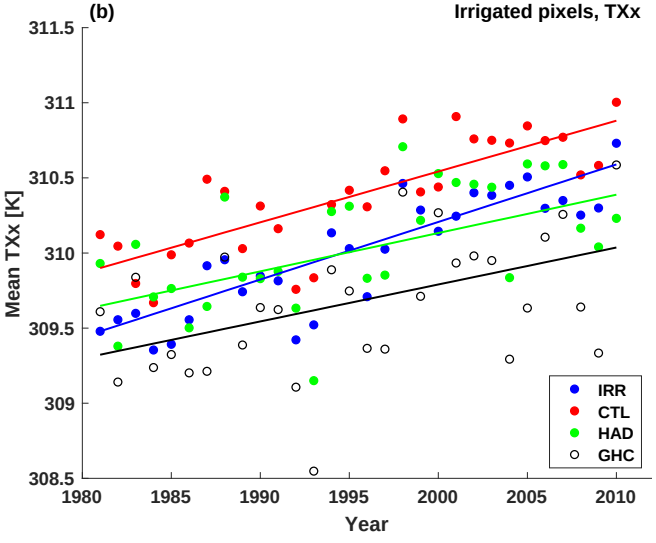


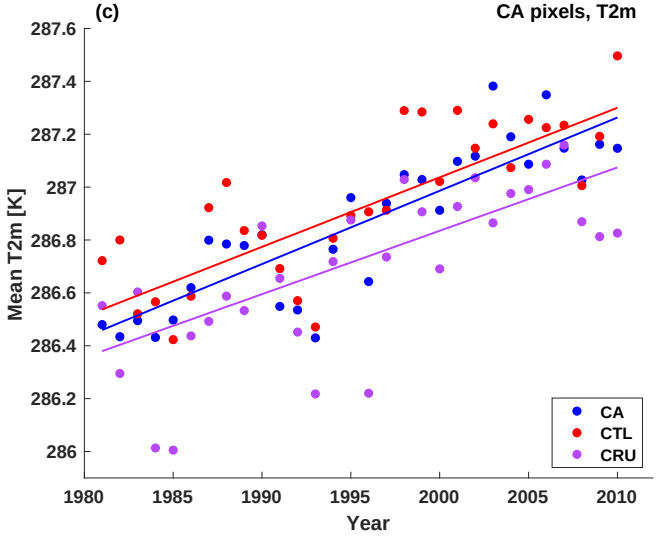


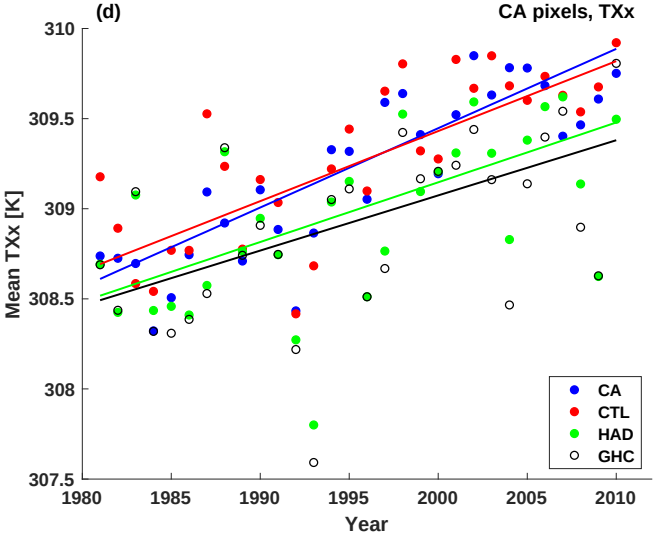

https://doi.org/10.5194/esd-2020-35
Preprint. Discussion started: 20 July 2020


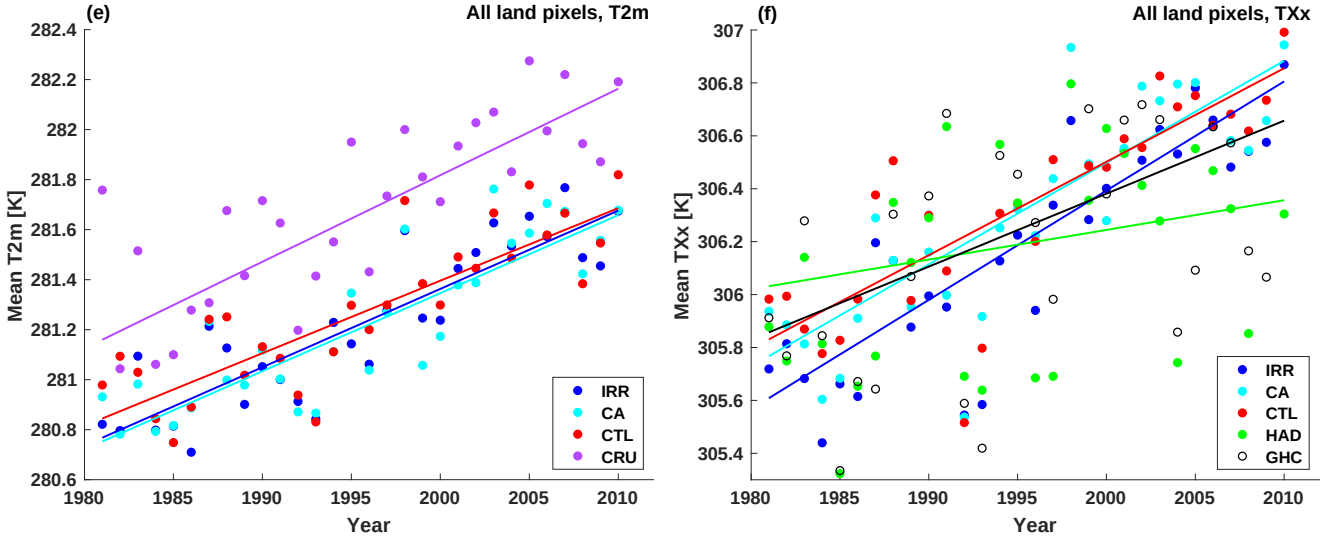


585 **Figure 4. Spatial average of the warming rates over irrigated pixels for $T_{2m}$ (a, c and e) and TXx (b, d and f) for the CESM ensembles and observations. For irrigated pixels (a-b), CA pixels (c-d), and (e-f) all land pixels. Legend: CTL (red), IRR (blue), CA (cyan), CRU (purple), HadEX2 (green), and GHCNDEX (black).**

https://doi.org/10.5194/esd-2020-35
Preprint. Discussion started: 20 July 2020


Earth System Dynamics
Discussions
Open Access
EGU

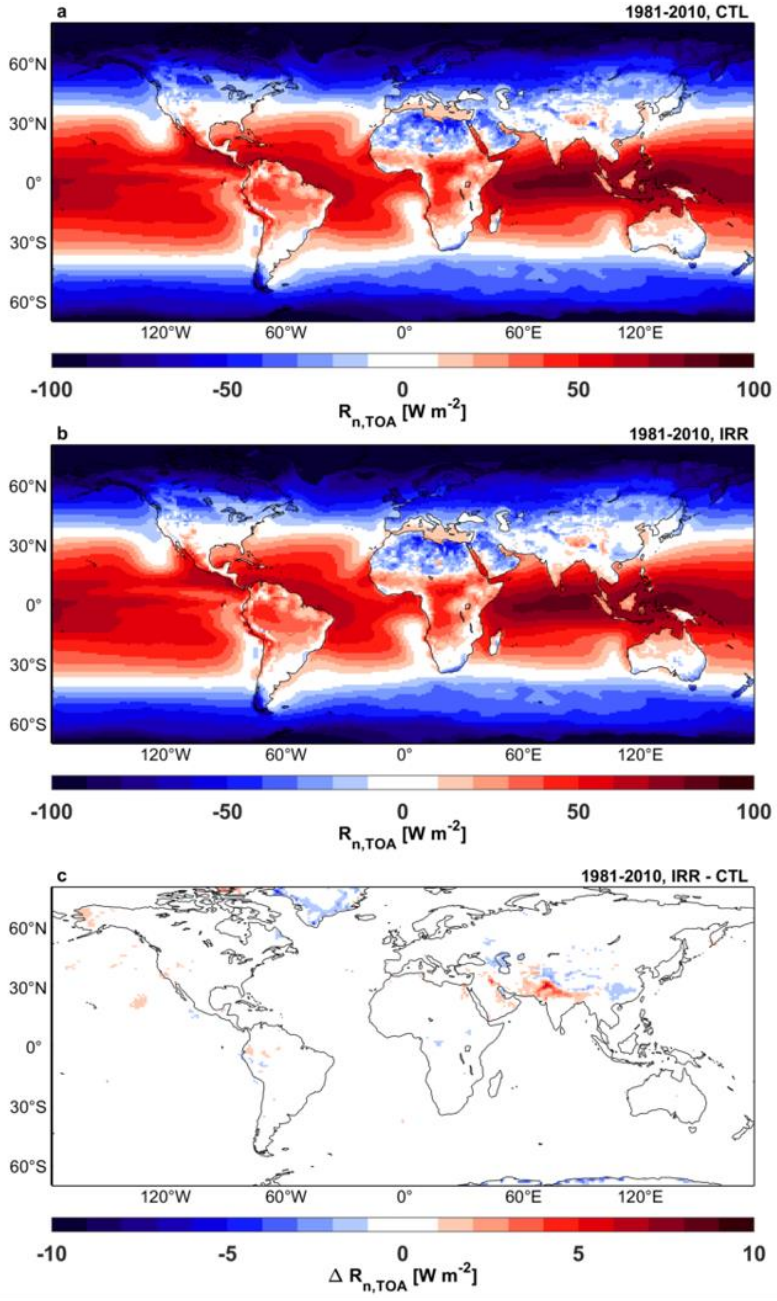


590

**Figure 5. Top-of-atmosphere (TOA) net radiation $R_{n,TOA}$ [W $m^{-2}$] in (a) the CTL ensemble and (b) the IRR ensemble. (c) Impact of irrigation on $R_{n,TOA}$. Difference map is based on the ensemble mean of each experiment for 1981–2010.**

https://doi.org/10.5194/esd-2020-35
Preprint. Discussion started: 20 July 2020


Earth System Dynamics
Discussions
Open Access
EGU

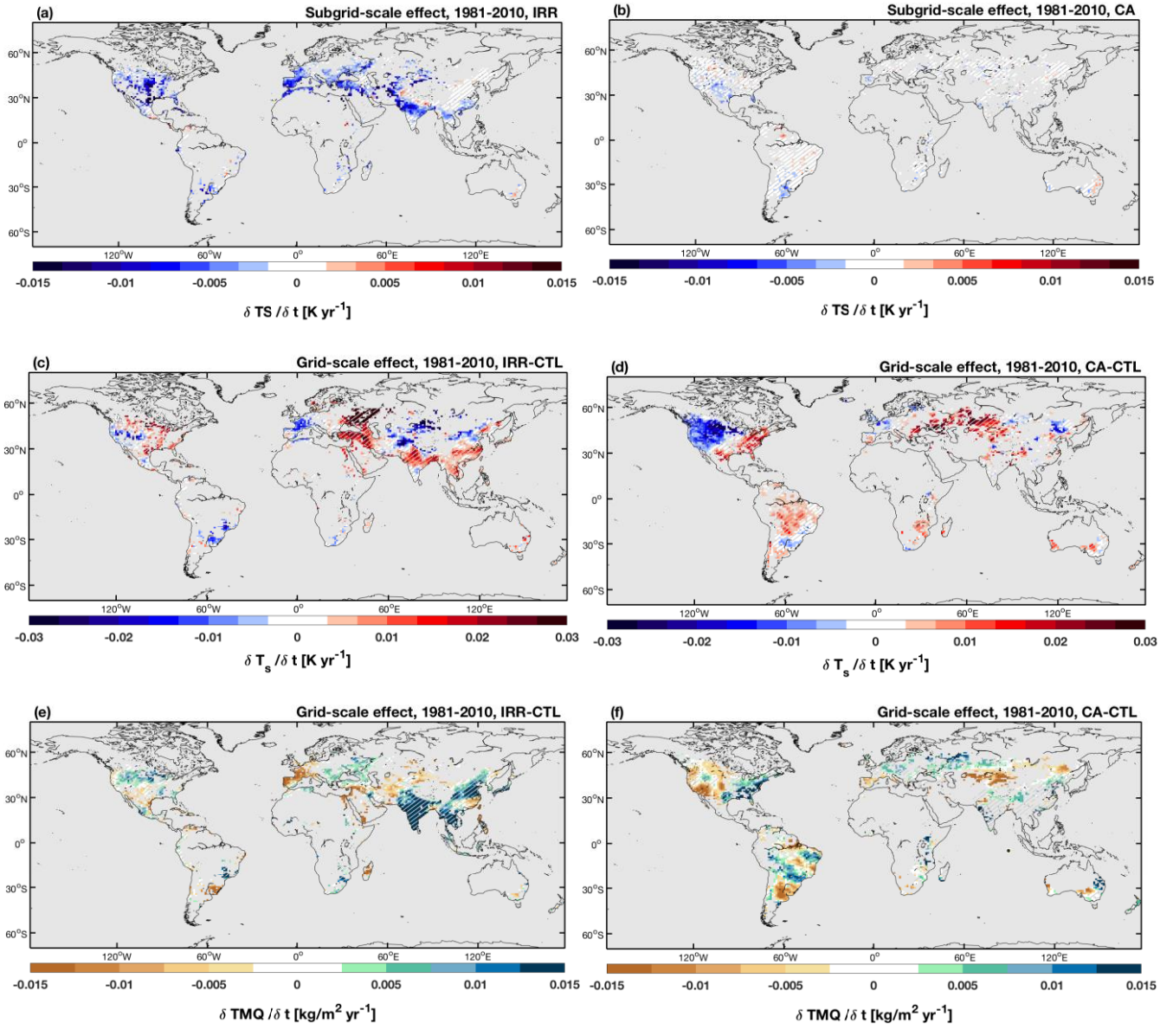


595

https://doi.org/10.5194/esd-2020-35
Preprint. Discussion started: 20 July 2020


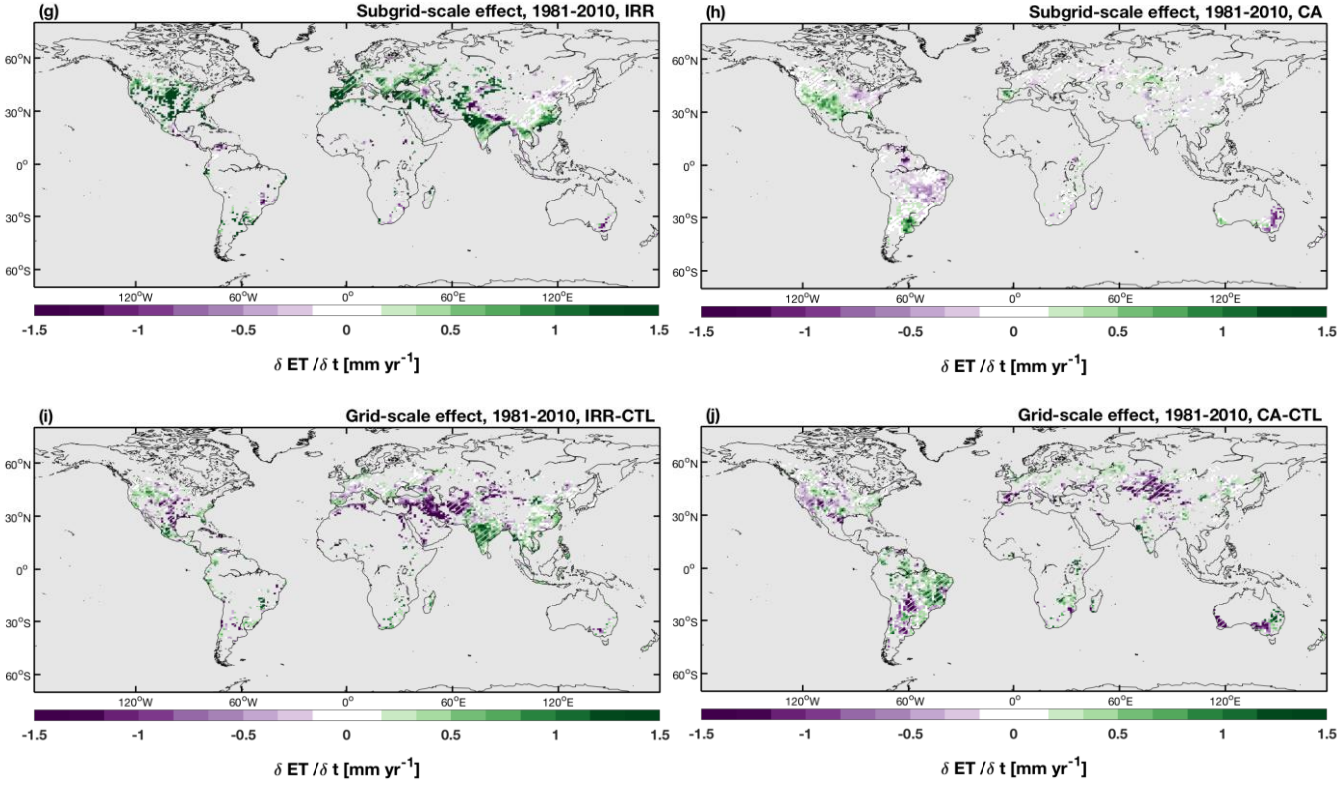


**Figure 6. Subgrid-scale differences between the irrigated and rainfed crop tile in the IRR ensemble (irrigated minus rainfed) (a and g) and between CA and conventionally managed (CM) crops (CA minus CM) (e and h). For $T_s$ (a-b) and ET (g-h). Grid-scale differences between the CTL and IRR ensemble (IRR minus CTL) (c, e and i) and between CA and conventionally managed (CM) crops (CA minus CM) (b, f and h). For $T_s$ (c-d), ET (i-j) and TMQ (e-f), displayed over irrigated/CA pixels for comparative purposes. Differences are based on the ensemble mean warming trends of each experiment for 1981–2010. Hatching denotes less than 10% change induced by the model on mean warming trends of lumped ensemble members.**

https://doi.org/10.5194/esd-2020-35
Preprint. Discussion started: 20 July 2020


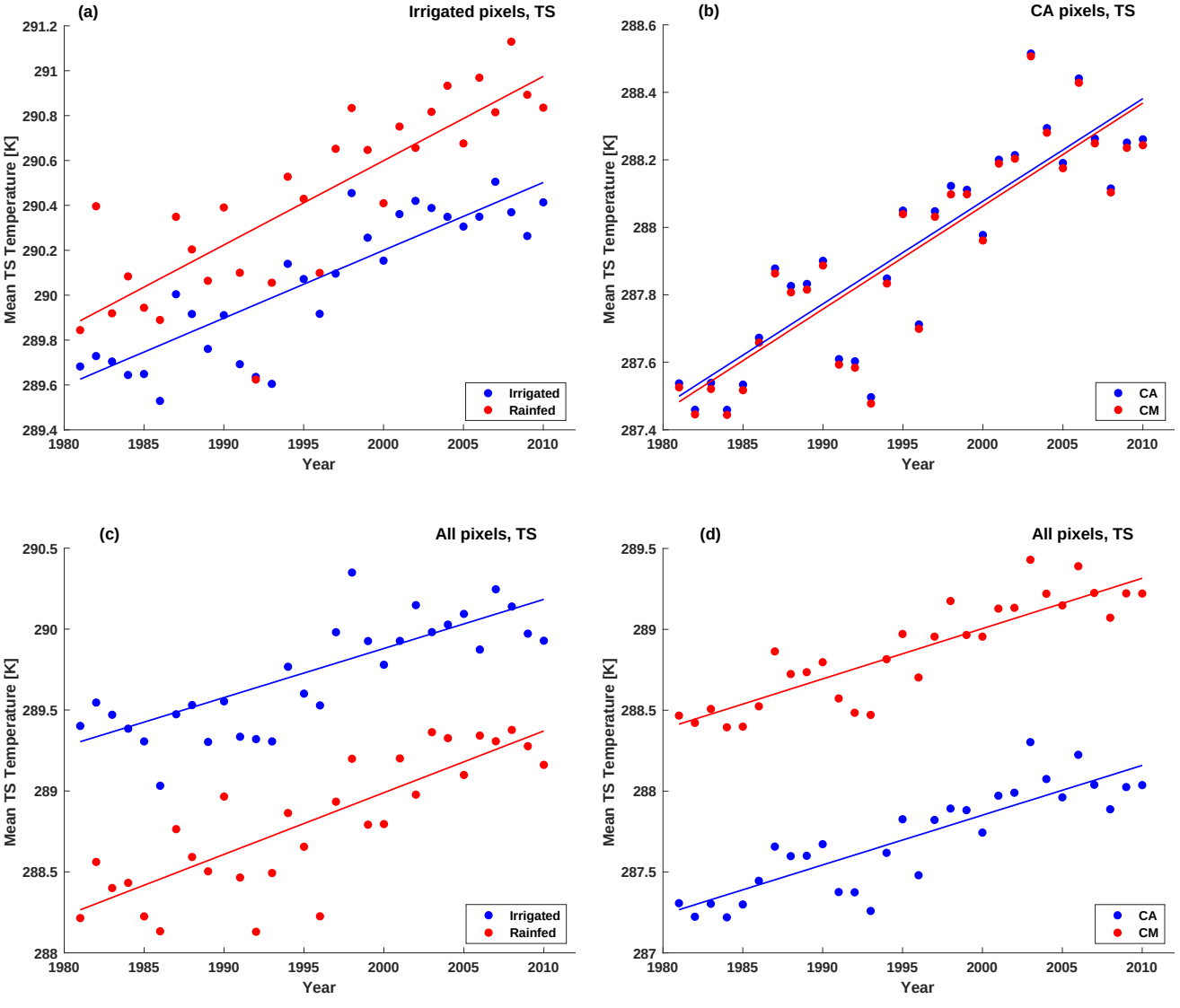


**Figure 7. Spatial average of the Ts warming rates over (a) irrigated pixels for the irrigated and rainfed crop tiles and over (b) CA pixels for the CA and CM crop tiles. For (a) and (b), the regions where less than 50% of the land pixels did not contain a value were excluded. Spatial average of the Ts warming rates for (c) the irrigated and rainfed crop tiles over all pixels and (d) the CA and CM crop tiles over all pixels. For all land pixels (c and d), the minimum number of land pixels that needed to contain a value in order to be retained in the analysis was 15%.**

https://doi.org/10.5194/esd-2020-35
Preprint. Discussion started: 20 July 2020


Earth System Dynamics Discussions

**Table 1. Bias and Spatial RMSE of the Ensemble Mean Warming Trends of the CTL, IRR and CA Experiments Versus the Warming Trends of the Observational Products[a].**

| | All land bias | | | Irrigated land bias | | CA land bias | | All land RMSE | | | Irrigated land RMSE | | CA land RMSE | |
|---|---|---|---|---|---|---|---|---|---|---|---|---|---|---|
| **Physical Quantity (Units)** | **CTL** | **IRR** | **CA** | **CTL** | **IRR** | **CTL** | **CA** | **CTL** | **IRR** | **CA** | **CTL** | **IRR** | **CTL** | **CA** |
| CRU $T_{2m}$ (K yr$^{-1}$) | -0.006 | -0.004 | -0.004 | -0.003 | 0.001 | 0.002 | 0.004 | 0.027 | 0.025 | 0.027 | 0.020 | 0.019 | 0.018 | 0.017 |
| GHCNDEX *TXx* (K yr$^{-1}$) | 0.024 | 0.030 | 0.027 | 0.009 | 0.013 | 0.006 | 0.011 | 0.107 | 0.111 | 0.110 | 0.078 | 0.082 | 0.124 | 0.125 |
| HadEX2 *TXx* (K yr$^{-1}$) | 0.007 | 0.013 | 0.010 | 0.008 | 0.012 | 0.008 | 0.013 | 0.135 | 0.135 | 0.136 | 0.121 | 0.122 | 0.086 | 0.087 |

[a]Regions with an observational coverage below 50% are excluded.

**Table 2. Impact of Irrigation and CA on Various Climatological Values (IRR Minus CTL and CA Minus CTL for Grid-Scale, $IRR_{SUB}$ Minus RAIN and $CA_{SUB}$ Minus CM for Subgrid-Scale)[a].**

| | | Irrigated Land | | | CA Land | | |
|---|---|---|---|---|---|---|---|
| | Physical Quantity (Units) | CTL | IRR | ABS | CTL | CA | ABS |
| **Grid-scale** | $T_{2m}$ (K yr$^{-1}$) | 0.026 | 0.030 | 0.004[c] | 0.026 | 0.028 | 0.002[c] |
| | TXx (K yr$^{-1}$) | 0.034 | 0.038 | 0.004[c] | 0.039 | 0.044 | 0.005[c] |
| | $T_S$ (K yr$^{-1}$) | 0.009 | 0.010 | 0.001[c] | 0.016 | 0.015 | -0.001[c] |
| | Physical Quantity (Units) | RAIN | $IRR_{SUB}$ | ABS | CM | $CA_{SUB}$ | ABS |
| **Subgrid-scale[b]** | $T_S$ (K yr$^{-1}$) | 0.038 | 0.030 | -0.008[c] | 0.031 | 0.030 | -0.001[c] |
| | ET (mm yr$^{-1}$) | 0.286 | 0.939 | 0.653[c] | 0.182 | 0.265 | 0.083 |

[a]ABS denotes the absolute change of each given quantity.

[b]Regions with a coverage below 25% are excluded. For grid-scale calculations, regions with a coverage below 50% are excluded.

[c]The changes significant at the 1% significance level (two-sided Wilcoxon signed rank test on ensemble mean slopes for irrigated/CA pixels.